Fermi Surface, Ground-State Electronic Structure, and Positron Experiments in $YBa_2Cu_3O_7$

A. Bansil,[1] R. Pankaluoto,[2] R. S. Rao,[2] P. E. Mijnarends,[3] W. Długosz,[1] R. Prasad,[1](a) and L. C. Smedskjaer[4]

[1]*Department of Physics, Northeastern University, Boston, Massachusetts 02115*
[2]*Physics Department, Tampere University of Technology, Tampere, Finland*
[3]*Netherlands Energy Research Foundation ECN, 1755 ZG Petten, The Netherlands*
[4]*Argonne National Laboratory, Argonne, Illinois 60439*

(Received 29 August 1988)

We present calculations of electron-positron momentum density in $YBa_2Cu_3O_7$ based on band theory in the local-density approximation. Theoretical predictions are in semiquantitative accord with the corresponding two-dimensional positron-annihilation angular-correlation measurements. These results indicate that the conventional local-density-approximation band-theory picture provides a reasonable description of the ground-state electronic structure and the Fermi surface of $YBa_2Cu_3O_7$. Several Fermi-surface–related features are suggested in the positron spectra for the first time.

PACS numbers: 74.70.Vy, 71.25.Hc, 78.70.Bj

Two-dimensional angular correlation of annihilation radiation (2D-ACAR) positron experiments have recently been reported on $YBa_2Cu_3O_7$ single crystals.[1,2] These measurements are of considerable interest because they can in principle help resolve important current questions concerning the existence of the Fermi surface in this material, and the extent to which the ground-state electronic structure is described by the conventional local-density-approximation (LDA) band-theory framework.[3] In view of the complexity of the 2D-ACAR spectra, however, a proper interpretation of the measurements requires a parallel theoretical computation of the two-photon momentum density $\rho_{2\gamma}(\mathbf{p})$. In this Letter, we present LDA band-theory calculations of $\rho_{2\gamma}(\mathbf{p})$ in $YBa_2Cu_3O_7$ and compare the results with the corresponding 2D-ACAR measurements. These are the first momentum-density computations reported in a high-T_c material.

We focus on the 2D projection of $\rho_{2\gamma}(\mathbf{p})$ along the crystal c axis since the band theory predicts nearly cylindrical Fermi surfaces oriented along this axis.[4,5] Hence, we expected the c projection to be the most sensitive in delineating the Fermi surface. Furthermore, we chose to carry out detailed initial computations along the YS and XS symmetry lines in the Brillouin zone because all major Fermi surfaces were expected to be "visible" along these directions.[6]

In the independent-particle momentum the 2γ momentum density $\rho_{2\gamma}(\mathbf{p})$ is given by

$$\rho_{2\gamma}(\mathbf{p})=\sum_{\mathbf{k},j} f(e_{\mathbf{k},j})\left|\int \exp(-i\mathbf{p}\cdot\mathbf{r})\psi_{\mathbf{k},j}(\mathbf{r})\phi_+(\mathbf{r})d\mathbf{r}\right|^2 . \tag{1}$$

Here, $\phi_+(\mathbf{r})$ and $\psi_{\mathbf{k},j}(\mathbf{r})$ denote the positron (e^+) and electron (e^-) wave functions, respectively. The Fermi-Dirac distribution function $f(E_{\mathbf{k},j})$ restricts the summation in Eq. (1) to occupied e^- states labeled by Bloch wave vectors $\mathbf{k}$ and band indices j. A 2D-ACAR experiment measures the 2D projection of $\rho_{2\gamma}(\mathbf{p})$ along a specific direction in momentum space, i.e.,

$$N_{2\gamma}(p_x,p_y)=\int_{-\infty}^{+\infty} dp_z\, \rho_{2\gamma}(p_x,p_y,p_z) . \tag{2}$$

Our theoretical treatment is based on the use of nonoverlapping muffin-tin potentials (including "empty" spheres) to represent the crystal potential.[7] The form of $\rho_{2\gamma}(\mathbf{p})$ for a lattice with basis may be described most simply in terms of the formula for the electron momentum density $\rho(\mathbf{p})$,[8-10]

$$\rho(\mathbf{p})=-\frac{(4\pi)^2}{\tau}\sum_j \frac{f(E)}{(E-p^2)^2}\frac{|\sum_\mu \exp(-i\mathbf{p}\cdot\mathbf{b}_\mu)\sum_L \bar{C}_{L\mu}(\mathbf{k})s_{l\mu}(p,E)\cot\eta_{l\mu}Y_L(\mathbf{p})|^2}{\sum_{\mu\nu}\sum_{LL'}\bar{C}_{L\mu}(\mathbf{k})\dot{M}^{\mu\nu}_{LL'}\bar{C}_{L'\nu}(\mathbf{k})} . \tag{3}$$

Here, all vectors and matrices are in the space of angular momentum and basis atom indices $L\equiv(l,m)$ and μ, and are to be evaluated at the energies $E=E_{\mathbf{k},j}$ of the Bloch levels at the reduced wave vector $\mathbf{k}$. $Y_L(\mathbf{p})$ is the Lth real spherical harmonic, τ is the unit-cell volume, $\mathbf{b}_\mu$ denotes the position and $\eta_{l\mu}$ the lth phase shift of the μth atom. The $s_{l\mu}(p,E)$ are smoothly varying functions involving the solutions of the radial Schrödinger equation for the μth muffin-tin potential. The remaining quantities are the Korringa-Kohn-Rostoker matrix M and its eigenvectors $\bar{C}_{L\mu}(\mathbf{k})$. They satisfy the secular equation $MC=0$.

The momentum density of the positron in its ground state ($\mathbf{k}=0$) is given by a formula similar to Eq. (3), except that in this case there is no summation over j. Keeping Eq. (1) in mind, $\rho_{2\gamma}(\mathbf{p})$ is then obtained straightforwardly as a convolution of the e^- and e^+ momentum-density functions.[11]

In implementing the theory, we first obtained the self-consistent LDA ground-state electronic structure using the linear-muffin-tin-orbital–atomic-sphere-approximation scheme, including semirelativistic corrections.[12] Perovskite-based orthorhombic-lattice-structure data of Ref. 13 were used. In addition to thirteen atoms in the unit cell of $YBa_2Cu_3O_7$, we inserted two "empty" spheres to account for the vacancies in the Y planes and the row of vacancies along the b axis. The self-consistency cycles were iterated to a high degree of convergence of various parameters (including Fermi energy, energy bands, and total charge around every site in the unit cell); the final cycles employed a 256-point mesh in the irreducible $\frac{1}{8}$th of the Brillouin zone. The self-consistent charge densities were used to construct one-particle e^- and e^+ muffin-tin potentials; exchange was excluded from the positron potential. These potentials were then used to obtain $\rho(\mathbf{p})$ and $\rho_{2\gamma}(\mathbf{p})$ and the associated 2D distributions via Eqs. (1)–(3); all valence bands (their number varying between 45 and 49) were summed in computing the momentum density.

The final band structure, shown in Fig. 1, is in good accord with the linearized-augmented-plane-wave results.[4,5] The Fermi surface in $YBa_2Cu_3O_7$ consists of four sheets: (i) a pair of closely placed S-centered hole sheets arising primarily from states in the Cu-O planes, which possess the shape of inner and outer surfaces of a "barrel" (marked $B_{1x},B_{2x},B_{1y},B_{2y}$ in Fig. 1); (ii) a sheet associated with the Cu-O chain band, which is completely occupied along ΓX but is almost empty along ΓY, and thus yields an electron "ridge" running along ΓX (points R_x,R_Γ); (iii) a rather complicated hole sheet related to an almost filled heavy-mass band which straddles the Fermi energy, and yields a hole "pillbox" around S (P_x,P_y), and a hole "butterfly" (F_1,F_2) along ΓY. Our Fermi surface is in good accord with other band structures, although small differences exist between vari-

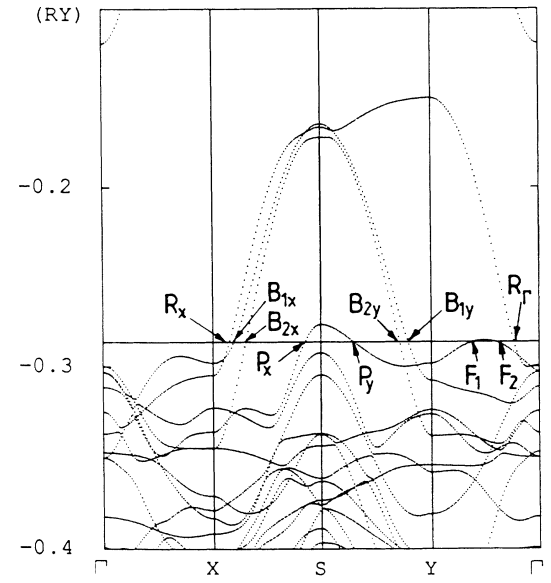

FIG. 1. Energy bands in $YBa_2Cu_3O_7$ along principal symmetry directions. Points where the Fermi energy (horizontal line) crosses various bands are marked.

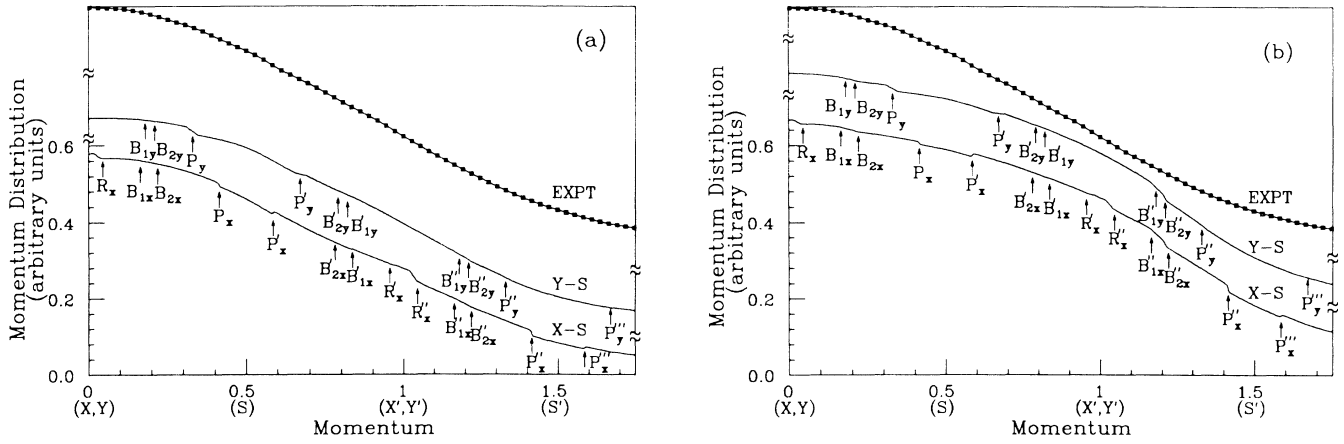

FIG. 2. (a) $N_{2\gamma}(p_x,p_y)$ and (b) the associated electron momentum distribution $N(p_x,p_y)$ obtained from Eq. (1) with $\phi_+=1$. To show the Fermi-surface related structures (R_x,B_{1x}, P_x, etc.) and the associated images in the higher Brillouin zones (R'_x,B'_{1x},B''_{1x}, etc.) clearly, theoretical curves along YS and XS are shown without smoothing. The experimental 2D-ACAR spectrum for a twinned single crystal along YS (or equivalently along XS) is shown in both (a) and (b). Momentum is given in scaled units where $p=0$ corresponds to the point X (and Y), and the reciprocal unit-cell dimension along XS (and YS) equals 1.0, permitting XS and YS results to be shown together on a convenient scale.

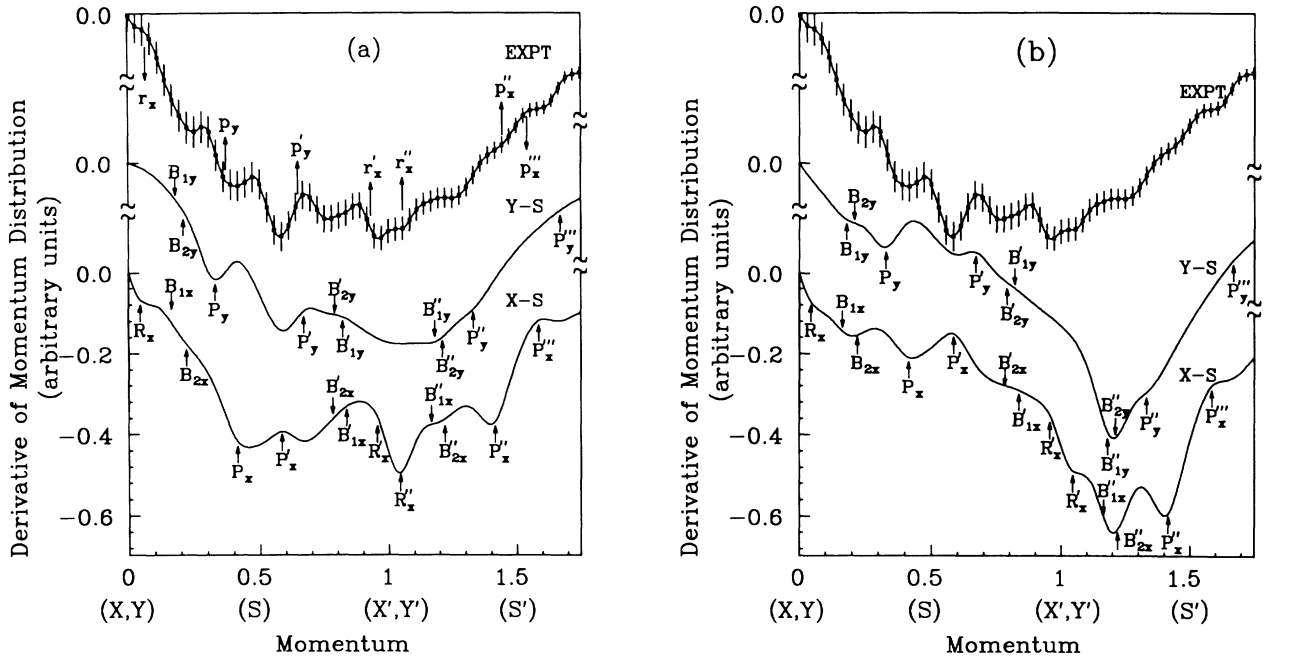

FIG. 3. Derivatives of the spectra shown in Figs. 2. (a) $dN_{2\gamma}/dp$ and (b) dN/dp. Theoretical derivatives were taken after convoluting the distributions of Fig. 2 with a Gaussian of FWHM = 0.8 mrad, which corresponds to the effective experimental resolution. Various features marked on the experimental curve are discussed in the text. Markings on the theoretical curves and the momentum scale are as in Fig. 2.

ous calculations, especially with respect to relatively smaller features associated with the heavy-mass band.

We discuss our momentum-density results now. In comparing theory with experiment, note that since measurements involved twinned crystals, the measured spectra along XS (or equivalently YS) would reflect features of the calculations along XS as well as YS.[14] Figure 2(a) shows that the width and shape of theoretical $N_{2\gamma}(\mathbf{p})$ curves along XS and YS are in excellent accord with measurements.[15] In contrast, the calculated e^- momentum distribution in Fig. 2(b) (without the positron) is much broader than the measured spectra. Despite the integration along the c axis [cf. Eq. (2)], clear signatures of the Fermi surfaces are seen in Fig. 2; the presence of images of the Fermi surface at higher momenta is especially striking. These results are related to the cylindrical shape of the Fermi surfaces, suggesting that the 2D-ACAR experiment would be more useful in studying Fermi surfaces in low-dimensional systems than has usually been assumed.

To enhance structure, Fig. 3(a) compares the derivatives of the distributions of Fig. 2; the calculated curves have been smoothed to reflect the effective experimental resolution.[16] The overall accord between calculations and measurements in Fig. 3(a) is remarkable; here again if the positron is not included in the calculations [Fig. 3(b)], the agreement is quite unsatisfactory.

The specific Fermi-surface features in the spectra may be interpreted as follows from Fig. 3(a). By scanning the curves between p values of 0.3 and 0.7 unit, we see that the measured and calculated curves are very similar in shape; in particular, the occurrence of the pillbox radius P_y at the minimum in the YS curve suggests that this radius may be identified as the feature p_y where the experimental curve begins the broad minimum around $p = 0.4$ unit; the image p_y' of this radius is similarly suggested in the measurements. The corresponding signatures along XS (P_x, P_x') are less prominent and would appear to be more difficult to identify. The images P_y'' and P_y''' of the pillbox on the other hand are seen to be weak, but P_x'' and P_x''' by contrast lead to stronger features, indicating that shoulders p_x'' and p_x''' in the experiment may be associated with the size of the pillbox sheet along XS.

The electron-ridge surface and its images (R_x, R_x', R_x''), present only along XS, lead to the characteristic drop followed by a plateau near $p = 0$ and to a dip near $p = 1.0$. If the ridge were somewhat broader, the dip near $p = 1.0$ would be expected to yield two discernible features arising from R_x' and R_x''. Note that along YS the calculated curve around $p = 1.0$ is quite featureless. Keeping these remarks in mind, we suggest associating r_x with the electron-ridge dimension along XS, and r_x' and r_x'' to be the images of the same in the measurements. In Ref. 1, the electron sheets were not possible to identify in the absence of the calculated spectra.

We turn finally to the pair of barrel sheets. Here the calculations yield a rather weak feature between $p=0.0$ and $p=0.5$ (B_{1x},B_{2x}) compared to the measurements in Fig. 3(a). A dip is, however, seen in the e^- momentum density [Fig. 3(b)]; this may suggest that the matrix elements connecting these states with the e^+ wave function should be somewhat stronger than is implicit in our calculations. The images of the barrel orbits (e.g., B'_{1x},B'_{2x},B''_{1x},B''_{2x}) also do not appear to leave any clear signatures in the calculated spectra. Our e^+ state is fairly delocalized and couples quite well with the Cu-O chains and the heavy-mass band, but not so well with the Cu-O plane bands.[17]

It is clear that other correlations between measurements and calculations could be established, especially in a higher-resolution experiment. Noteworthy also is the fact that many spectral features are not related with any specific Fermi surface but reflect the complex nature of the matrix elements (e.g., the peak at about $p=0.4$ and the dip at about $p=0.6$ in the YS curve).[18]

In conclusion, the semiquantitative accord between the measured and calculated spectra seen here indicates that the conventional LDA band-theory framework provides a reasonable description of the ground state and the Fermi surface of $YBa_2Cu_3O_7$.

We acknowledge important discussions with R. Benedek and S. Kaprzyk, and thank M. Pessa and K. Kaski for support and encouragement. This project is supported by DOE Grants No. DE-FGO2-85ER45223 and No. W-31-109-Eng-38, the Academy of Finland, the U.S.–Finland Program of NSF, and an NSF grant via the NBS Synchrotron Ultraviolet Radiation Facility, and benefited from the allocation of time on the ER-Cray at LLNL.

---

[a]Permanent address: Department of Physics, Indian Institute of Technology, Kanpur, India.

[1]L. C. Smedskjaer, J. Z. Liu, R. Benedek, D. G. Legnini, D. J. Lam, M. D. Stahulak, H. Claus, and A. Bansil, Physica (Amsterdam) **156C**, 269 (1988).

[2]L. Hoffmann, A. A. Manuel, M. Peter, E. Walker, and M. A. Damento, Europhys. Lett. **6**, 61 (1988).

[3]For recent comments on theories of high-T_c superconductivity, see, e.g., P. W. Anderson, Science **235**, 1196 (1987); C. M. Varma, S. Schmitt-Rink, and E. Abrahams, Solid State Commun. **62**, 681 (1987). For effects of correlations on the momentum density, see W. Metzner and D. Vollhardt, Phys. Rev. B **37**, 7382 (1988).

[4]J. Yu, S. Massidda, A. J. Freeman, and D. D. Koelling, Phys. Lett. A **122**, 203 (1987).

[5]H. Krakauer, W. E. Pickett, and R. E. Cohen, to be published.

[6]The ΓS line would be another suitable choice.

[7]The agreement between Fig. 1 and linearized-augmented-plane-wave band structures indicates that our approach is reasonable. The neglected non-muffin-tin corrections are being considered.

[8]P. E. Mijnarends and A. Bansil, Phys. Rev. B **13**, 2381 (1976).

[9]P. E. Mijnarends and L. P. L. M. Rabou, J. Phys. F **16**, 483 (1986).

[10]Equation (3) differs from Eq. (22) of Ref. 9 in that the latter contains factors of squares of muffin-tin radii, r_μ^2, in the denominator and the numerator. Equation (22) of Ref. 9 is incorrect and leads to unphysical results near free-electron poles for basis atoms of different radii.

[11]The neglected effects of e^--e^+ correlations are not expected to influence the shape of 2D-ACAR curves substantially.

[12]We have used Skriver codes [H. L. Skriver, *The LMTO Method,* Springer Series in Solid-State Sciences Vol. 41 (Springer-Verlag, Berlin, 1984)] modified somewhat to treat the orthorhombic lattice.

[13]M. A. Beno, L. Soderholm, D. W. Capone, II, D. G. Hinks, J. D. Jorgensen, I. K. Schuller, C. U. Segre, K. Zhang, and J. D. Grace, Appl. Phys. Lett. **51**, 57 (1987).

[14]It is not sensible to average the calculate spectra along XS and YS for comparison with experiment for several reasons. Along these two directions, the zone dimensions are different in the calculations, as is the instrumental response in the measurements; measured and calculated Fermi-surface radii along the two directions will also in general differ by different amounts.

[15]While we present our own 2D-ACAR data in Figs. 2 and 3, the experiments of Refs. 1 and 2 are in substantial agreement.

[16]See Ref. 1 for experimental details. While caution is necessary in taking derivatives, an analysis of error propagation shows that our procedures do not introduce any artificial structures in the experimental spectra of Fig. 3 beyond the indicated error bars.

[17]See also, von Stetten *et al.* [Phys. Rev. Lett. **60**, 2198 (1988)], and Jean *et al.* [Phys. Rev. Lett. **60**, 1069 (1988)].

[18]Momentum density even in the insulating state is thus expected to be anisotropic and contain structures due to the contribution of fill bands and/or positron wave-function effects; such structures will tend to disappear upon LCW (Lock-Crisp-West) folding.